Temperature dependence of the characteristic length scale for glassy dynamics: Combination of dielectric and specific heat spectroscopy

Allisson Saiter, L. Delbreilh, H. Couderc, K. Arabeche, A. Schönhals, J.-M. Saiter

Temperature dependence of the characteristic length scale for glassy dynamics: Combination of dielectric and specific heat spectroscopy

A. Saiter,[1,*] L. Delbreilh,[1] H. Couderc,[1] K. Arabeche,[1] A. Schönhals,[2] and J.-M. Saiter[1]
[1]*L'Equipe de Caractérisation des Amorphes et des Polymères (L'ECAP), Institut des Matériaux de Rouen, FED4114, Faculté des Sciences, Université de Rouen, Site du Madrillet, 76801 Saint Etienne du Rouvray Cedex, France*
[2]*BAM Federal Institute for Materials Research and Testing, Unter den Eichen 87, 12205 Berlin, Germany*
(Received 19 February 2010; published 22 April 2010)

The temperature dependence of characteristic length scales associated to the glass transition such as the cooperativity length scale introduced by Adam and Gibbs [cooperative rearranging region (CRR)] or the dynamic heterogeneity as estimated from the four point correlation function χ_4, is at the center of large interests. Broadband dielectric spectroscopy and temperature modulated differential scanning calorimetry allow to study the CRR size temperature dependence in the temperature range of ergodicity loss for glass-forming liquids, starting from the onset of cooperativity in the crossover region down to the glass transition temperature. Furthermore, the correlation between these two techniques allows to explore a large frequency range (from 1 mHz to 10 MHz). The goal of this work is to follow the cooperativity evolution along the Arrhenius plot for two different polymeric systems: poly(ethylene 1,4-cyclohexylenedimethylene terephthalate glycol) and poly(bisphenol A carbonate).

DOI: 10.1103/PhysRevE.81.041805 PACS number(s): 61.25.H−, 76.60.−k, 64.70.pj, 77.84.Jd

I. INTRODUCTION

If a glass-forming liquid is cooling down a dramatic increase in the viscosity and the structural (α)-relaxation times τ is observed. Decreasing the temperature at atmospheric pressure by a factor of 2, τ may increases by more than 14 orders of magnitude. This dramatic increase in the relaxation times with decreasing temperature can be most naturally interpreted assuming a cooperative behavior of the relevant molecular motions. Like in low molecular glass forming liquids in the polymeric glass formers, segmental dynamics are known to be cooperative [1,2] rearranging movements of a given structural unit are only possible if a certain number of neighboring units are also moving. These movements concern molecular fluctuations in a polymeric chain and a part of various molecular units belonging to neighboring chains. The extent of this cooperativity is assumed to increase with decreasing temperature and should be in the range of a few nanometers at the thermal glass transition. Adam and Gibbs [3] have introduced the notion of the cooperative rearranging region (CRR) defined as a subsystem, which can rearrange its configuration to another one, independently of its environment. Using this picture the temperature dependence of the relaxation time close to the thermal glass transition temperature T_g which obeys the empirical Vogel/Fulcher/Tammann (VFT) law [4–6] can be well described. For higher temperatures than T_g at a temperature T_B in the range $T_B/T_g \approx 1.2-1.3$ the temperature dependence of τ changes from this low temperature VFT behavior to a high temperature VFT law (see for instance Ref. [7] and literature quoted there). In parallel to the change in the temperature dependence of the relaxation rate also a change in the temperature dependence of the dielectric relaxation strength [8] is observed at T_B. Moreover in the same temperature range the localized Goldstein/Johari (genuine) β process which is regarded as a precursor of dynamic glass transition splits from the α relaxation (see Refs. [7,9] and literature quoted there). Although the temperature dependence of the relaxation time is still weak non-Arrhenius, it is widely discussed in the literature that T_B indicates the onset of cooperativity. It is also worth to note that the critical temperature predicted by the mode coupling theory to the glass transition [10] is quite close to T_B. According to this theory for temperatures above T_C or T_B the molecular motion can be described by a cage leaving-flow process which also leads to a non-Arrhenius temperature dependence of the relaxation rates.

Literature shows a great interest of scientists in determining the temperature dependence of such system cooperativity either by using the Adam and Gibbs theory [11–16], or by calculating a correlation number from the four point correlation function χ_4 [17–19]. In this work, we propose to use the fluctuation approach developed by Donth to estimate the size of the CRR also in its temperature dependence.

According to Donth *et al.* [20], the CRR volume can be calculated from the von Laue approach describing a system with a fluctuating temperature. Each CRR presents a fluctuating region of molecular mobility (and so relaxation time) and can be understood as a group of "sub-subsystems," called structural units, each one having its own glass transition temperature, and its own free volume, linked to its own relaxation time. The resulting glass transition temperature distribution can be experimentally obtained from temperature modulated differential scanning calorimetry (TMDSC) [21] or from broadband dielectric spectroscopy (BDS) [7]. According to this approach, the average volume of a CRR denoted as V_α can be estimated according to the following equation [1]:

$$V_\alpha = \frac{\Delta(1/C_v)}{\rho(\delta T)^2} k_B T_\alpha^2, \tag{1}$$

where T_α is the dynamic glass transition temperature, ρ the density at T_α, k_B the Boltzmann constant, δT the average

*Corresponding author.

TABLE I. Measured quantities in TMDSC and BDS experiments.

	TMDSC	BDS
Disturbance	Temperature T	Electric field E
Response	Entropy S	Polarization P
Material function	Entropy compliance $J_S^*(\omega)$	Dielectric susceptibility $\chi''(\omega)$

temperature fluctuation related to the dynamic glass transition of an average CRR. From the application of the fluctuation dissipation (or Callen-Welton) theorem [22,23] to heat capacity spectroscopy (HCS, with entropy S as extensive variable and temperature T as intensive variable) and approximating the loss part C'' of the complex heat capacity C^* as function of temperature at fixed frequency as a Gaussian, Donth has shown that the average temperature fluctuation δT corresponds to the standard deviation σ_T of the Gaussian [1].

The difference in reciprocal specific heat capacity at constant volume $\Delta(1/C_v)$ is determined at the dynamic glass transition temperature T_α from TMDSC data via the approximation

$$\Delta(1/C_v) \approx \Delta(1/C_p) = (1/C_p)_{glass} - (1/C_p)_{liquid}, \qquad (2)$$

where C_p is the specific-heat capacity at constant pressure.

The average CRR volume have been calculated for numerous organic polymers to study for example the influence of nanofiller content, the confinement effects due to the presence of crystalline phases, on the glass transition dynamics [12,24–26]. Recently, Schröter published a review article concerning the estimation of characteristic length scales or cooperativities for the α relaxation by the fluctuation approach from calorimetric data and put in evidence that it is an important tool in studying molecular mobility [27]. The number of particles per CRR noted N_α can be estimated by

$$N_\alpha = \frac{\rho N_A V_\alpha}{M_0} = \frac{N_A \Delta(1/C_p)}{M_0 (\delta T)^2} k_B T_\alpha^2, \qquad (3)$$

where N_A is the Avogadro number and M_0 the molar mass of the relevant structural unit, in the considered case the molecular mass of the repeating unit. It worth to note that the number of segments N_α is one CRR do not belong to one polymeric chain but to many chains, because close to the glass transition a polymeric melt is a quite dense system.

As discussed above, the relaxation function or spectra at the dynamic glass transition (α relaxation) of glass forming liquids in general and polymers in a more special case, is much broader than the Debye function (single relaxation time) and has to be described by a relaxation time distribution function. Thus, the Arrhenius diagram representing the relaxation time as a function of temperature does not correspond to a single curve associated to a single function $\tau(T)$, but to a so-called dispersion zone [1]. Assuming the time/temperature equivalence and representing the sample in terms of an average CRR size, δT also represents the temperature range of this dispersion zone. From this viewpoint, HCS experiments such as the 3ω method [28–30], TMDSC [31,32] and ac chip calorimetry [33–35] allow to study the temperature dependence of the cooperativity length scale calculated at the corresponding dynamic glass transition temperature, this means along the trace of the dynamic glass transition in the Arrhenius plot [36,37]. All parameters of Eq. (3) can be determined by HCS for different frequencies ω or corresponding temperatures T_α.

The study of the α relaxation as function of the frequency or temperature leads to the determination of its characteristic parameters, in particular of the average temperature fluctuation δT and the dynamic glass transition temperature T_α. This enables the calculation of the temperature dependence of the CRR size in a wide temperature range, starting from the onset of cooperativity in the crossover region around T_B down to the thermal glass transition temperature T_g.

In order to explore a large frequency range (from 1 mHz to 10 MHz) it is useful to correlate the HCS method with BDS. There are several common and/or complementary features for the glass transition phenomenon studied by these two techniques:

(i) Both methods probe the dynamic glass transition by applying a periodic perturbation to the sample (a modulated temperature ramp in TMDSC and a periodic electrical field in BDS). These techniques allow to measure complex quantities: the complex heat capacity C_p^* for TMDSC and the complex dielectric permittivity ε^* for BDS consisting in corresponding real and imaginary parts (respectively C_p' and C_p'', ε', and ε'') [7,18].

(ii) From the point of view of the linear response theory both the complex permittivity and the complex heat capacity are generalized compliances. Therefore, both quantities can be compared directly.

(iii) The response forms: by TMDSC, the dynamic glass transition is traduced by a heat capacity step ΔC_p in the real part and a dissipative peak in the imaginary part. By BDS, the dynamic glass transition is traduced by a step called dielectric strength $\Delta\varepsilon$ and a peak in the imaginary part. ΔC_p and $\Delta\varepsilon$ are both linked to the amorphous phase quantity involved in the glass transition [4,6].

(iv) At each temperature, the glass forming liquids present a relaxation time distribution function. Using an Arrhenius diagram, these distributions are represented by a dispersion zone [1]. It is known that this dispersion zone broadens as the temperature increases. This is shown by a broadening and a loss peak shift toward higher temperatures as the frequency of the applied perturbation increases, which is observable by BDS [6] and by HCS experiments [21,38].

However, the measured quantities are different between these two experimental techniques (see Table I):

(i) The temperature T and the electric field E are the intensive variables

(ii) The entropy S and the orientation polarization P are the extensive variables

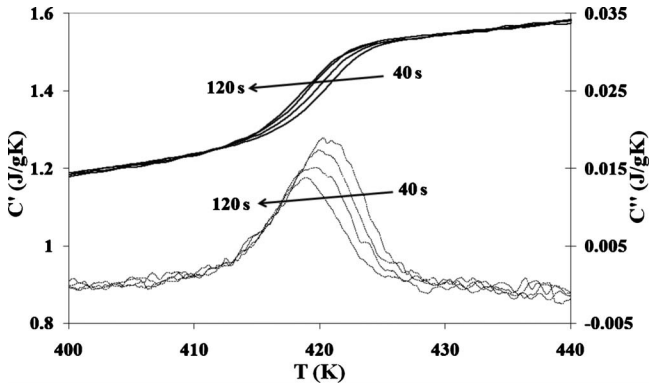

FIG. 1. Real part (C′) and loss part (C″) of the complex heat capacity C^* (t) versus temperature for PC for the different oscillation periods (40, 60, 90, and 120 s) at a cooling rate of q= −0,5 K/min, and an oscillation amplitude of 1 K.

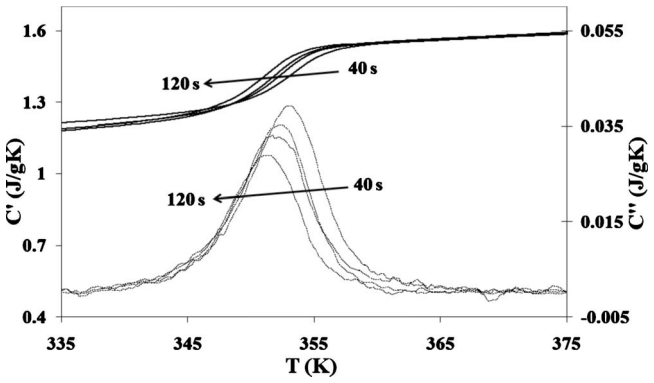

FIG. 2. Real part (C′) and loss part (C″) of the complex heat capacity C^* (t) versus temperature for PETg for the different oscillation periods (40, 60, 90, and 120 s) at a cooling rate of q= −0,5 K/min, and an oscillation amplitude of 1 K.

The Callen-Welton theorem application gives the following relations for TMDSC [1]:

$$G_T''(\omega) = \frac{\pi\omega\Delta T^2(\omega)}{k_B T}, \tag{4}$$

$$J_S''(\omega) = \frac{\pi\omega\Delta S^2(\omega)}{k_B T}, \tag{5}$$

G_T'' is the imaginary part of the complex temperature modulus $G_T^* = \frac{\partial T}{\partial S} = \frac{T}{c_v^*}$ and J_S'' the imaginary part of the complex entropy compliance $J_S^* = \frac{\partial S}{\partial T} = \frac{c_v^*}{T}$, and $\Delta T^2(\omega)$ and $\Delta S^2(\omega)$ are the respective spectral densities of temperature and entropy fluctuations and c_v^* the complex specific heat capacity at constant volume.

For BDS the equivalent relations are the following [6]:

$$M''(\omega) = \frac{\pi\omega\Delta E^2(\omega)}{k_B T}, \tag{6}$$

$$\chi''(\omega) = \varepsilon''(\omega) - 1 = \frac{\pi\omega\Delta P^2(\omega)}{k_B T}, \tag{7}$$

M'' is the imaginary part of the complex electric modulus $M^* = \frac{\partial E}{\partial P}$ and χ'' the imaginary part of the dielectric susceptibility $\chi^* = \varepsilon^* - 1 = \frac{\partial P}{\partial E}$, $\Delta E^2(\omega)$ and $\Delta P^2(\omega)$ are the respective spectral densities of the local electric field and the polarization. ε^* is the complex dielectric permittivity.

Combining Eqs. (4) and (7) yield

$$\frac{\Delta T^2(\omega)}{\Delta P^2(\omega)} = \frac{G_T''(\omega)}{\chi''(\omega)}, \tag{8}$$

Assuming that $G_T''(\omega)$ and $\chi''(\omega)$ can be factorized in an intensity factor and a spectral shape function of (ω)

$$G_T''(\omega) = G_0(T) \times f_T(\omega) \quad \chi''(\omega) = \chi_0(T) \times f_\chi(\omega). \tag{9}$$

It holds

$$\frac{\Delta T^2(\omega)}{\Delta P^2(\omega)} = \frac{G_0(T) \times f_T(\omega)}{\chi_0(T) \times f_\chi(\omega)}. \tag{10}$$

Provided that temperature and polarization fluctuations have approximately the same spectral shape function $f_T(\omega) \approx f_\chi(\omega)$, which seems to be a reasonable assumption, the width of the temperature fluctuations can be estimated from the width of polarization fluctuations.

The aim of this work is to follow the cooperativity evolution along the Arrhenius plot for two different polymeric systems poly(ethylene 1,4-cyclohexylenedimethylene terephthalate glycol) denoted as PETg and poly(bisphenol A carbonate) denoted as PC, and to compare the experimental dependencies with the theoretical ones on a large frequency domain. Furthermore, this work allows to confirm that temperature and polarization fluctuations have comparable spectral shape functions $f_T(\omega) \approx f_\chi(\omega)$.

II. EXPERIMENTAL

Amorphous PETg is provided by Eastman Chemical Co. Its monomer unit molar mass is 218 g/mol, its number average molecular weight is 26 000 g/mol, and its glass transition temperature is 350 K. PC is provided by general electrics. Its monomer unit molar mass is 192 g/mol, its number average molecular weight is 47 400 g/mol and its glass transition temperature is 418 K. The molecular weight of weight of both polymers is considerable high and above the critical molecular weight of ca. 10^4 g/mol below that chain end effects have to be considered. The samples are analyzed using TMDSC of thermal analysis (TA Q100). Calibration in temperature and energy is carried out using standard values of indium and zinc, and the specific heat capacities for each sample are measured using sapphire as a reference. For a detailed discussion see for instance reference [39]. The sample masses are chosen to be similar to the sapphire sample mass, i.e., approximately 20 mg. The TMDSC experiments were performed with an oscillation amplitude of 1 K, an oscillation period of 40, 60, 90, and 120 s and with a cooling rate of 0.5 K/min. The calibration is performed for each frequency. These experimental parameters give the best

"signal to noise" ratio obtained with the used apparatus. The samples sustain a thermal treatment at 400 and 470 K, for PETg and PC, respectively, during 10 min, in order to avoid thermal history effects.

Dielectric relaxation spectroscopy experiments are carried out in a parallel plate geometry using circular gold plated having a diameter of 20 mm. The Novocontrol Concept 40 ALPHA-analyzer interfaced to the sample by a broadband dielectric converter (BDC, Novocontrol) allows to obtain the complex dielectric permittivity under a nitrogen atmosphere isothermally in the frequency range from 10^{-1} to 10^{7} Hz. The temperature is varied between 193 and 433 K for PETg and between 400 and 470 K for PC, in consecutive increasing steps of 3 K and is controlled with a stability of $\Delta T = 0.1$ K (Novocontrol Quatro system controller BDS 1330).

The samples sustain a thermal treatment between the electrodes in order to improve the material/electrodes contact and to avoid thermal history effects. This treatment consists in annealing at 400 and 470 K, respectively for PETg and PC, during 10 min, followed by a cooling run at 10K/min to the start temperature.

III. RESULTS

From TMDSC, different signals are obtained: the total heat flow and the complex specific-heat capacity C^* [21,39] given by the following equation:

$$|C^*| = \frac{A_q}{\omega A_T} \times \frac{1}{m}. \tag{11}$$

Where A_q is the amplitude of the modulated heat flow, A_T the amplitude of the temperature, and m the sample mass. Due to the phase shift φ between the calorimeter response function (i.e., the total heat flow) and modulated temperature, two components C' (the in-phase component, real part) and C'' (the out-of-phase component or loss part) are calculated according to

$$C' = |C^*| \cos \varphi, \tag{12}$$

$$C'' = |C^*| \sin \varphi. \tag{13}$$

However, the raw phase lag, as given by the apparatus, must be carefully corrected for heat transfer effects [40,41] (between the sample and the thermocouple and in the sample itself) and also because of apparatus asymmetry [42].

Concerning BDS measurements, in the frequency domain, to remove the contributions of the conductivity from the α relaxation process a power law [43] and the Havriliak-Negami [44] function is used:

$$\varepsilon^*(\omega) = \frac{\sigma_0}{\varepsilon_0 \omega^s} + \varepsilon_\infty + \frac{\Delta\varepsilon}{[1 + (i\omega\tau)^\alpha]^\beta}, \tag{14}$$

where σ_0 is related to the conductivity contribution of mobile charge carriers, s is a fitting parameter and ε_0 is the permittivity of vacuum. ε_∞ is the unrelaxed dielectric permittivity, $\Delta\varepsilon$ the dielectric relaxation strength, τ the relaxation time, α and β the Havriliak-Negami parameters describing the symmetric and asymmetric broadening of the relaxation time distribution function, respectively. Contributions of a β relaxation due to localized motional processes at higher frequencies are removed from the α relaxation by applying a second HN function.

To have a consistent treatment for both TMDSC and BDS data the loss peaks are analyzed in the temperature domain using (for BDS the analyzed data are used as described above) a Gaussian law by a Levenberg-Marquardt iteration procedure

$$f''(T) = \frac{A}{\sigma_T \sqrt{2\pi}} \exp\left(\frac{T - T_\alpha}{\sigma_T}\right)^2, \tag{15}$$

where A corresponds to the peak area.

Figures 1 and 2 show the real and the loss part of the $C^*(T)$ for PC and PETg, respectively, measured by TMDSC at different frequencies. With increasing frequency, for both samples, the heat capacity step in C' and the loss peak maximum in C'', corresponding to the dynamic glass transition temperature T_α, shifts to higher temperatures when the frequency increases (i.e., when the oscillation period decreases as mentioned on the figures) as expected and observed in the literature [45]. A more careful inspection of these thermo-

TABLE II. TMDSC results on PC and PETg with different modulations periods. T_α is the dynamic glass transition temperature, equivalent to the loss peak maximum; σ_T is the Gaussian standard deviation of the loss peak; V_α and N_α are respectively the volume of an average CRR and the particle number in the average CRR.

Sample	Period (s)	T_α (K)	σ_T (K)	V_α (nm^3)	N_α
PC	40	420.3 ± 0.5	3.04 ± 0.05	26.4 ± 3	76 ± 7
PC	60	419.7 ± 0.5	2.99 ± 0.05	27.4 ± 3	79 ± 7
PC	90	419.3 ± 0.5	2.92 ± 0.05	28.7 ± 3	82 ± 7
PC	120	418.6 ± 0.5	2.75 ± 0.05	32.6 ± 3	93 ± 8
PETg	40	352.7 ± 0.5	2.89 ± 0.05	22.6 ± 2	79 ± 8
PETg	60	351.8 ± 0.5	2.81 ± 0.05	23.9 ± 2	84 ± 8
PETg	90	351.7 ± 0.5	2.86 ± 0.05	23.1 ± 2	81 ± 8
PETg	120	350.9 ± 0.5	2.78 ± 0.05	24.5 ± 2	86 ± 8

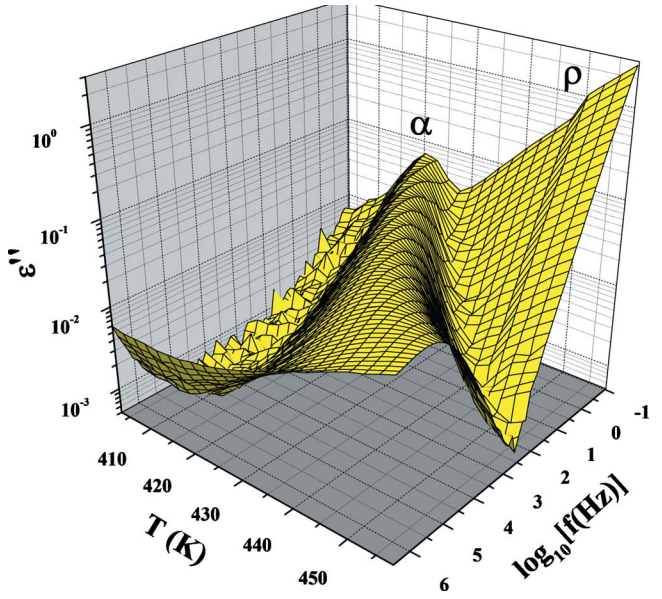

FIG. 3. (Color online) Dielectric loss versus frequency and temperature for PC.

grams give that for both samples the imaginary part of the specific heat capacity C″ show frequency independent low-temperature wings. As discussed in detail by Weyer *et al.* [46], this might be due to an interference between the measurement of the complex heat capacity (dynamic glass transition) and vitrification of the sample on cooling down to the thermal glass transition temperature (thermal glass transition). A disentanglement of both effects requires the application sophisticated models based on the Tool/Narayanaswamy/Moynihan treatment which is beyond the scope of this paper. Nevertheless on has to keep this in mind.

Also, the loss peak broadens with increasing frequency, leading to an increase in the standard deviation σ_T of the

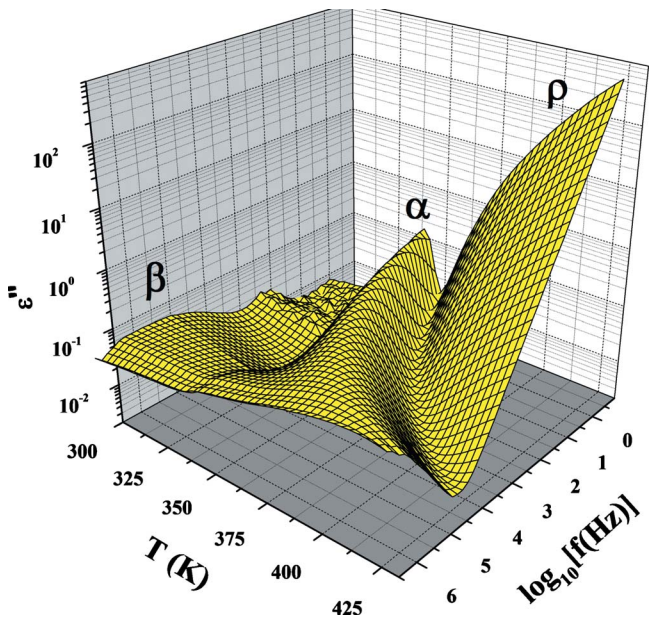

FIG. 4. (Color online) Dielectric loss versus frequency and temperature for PETg.

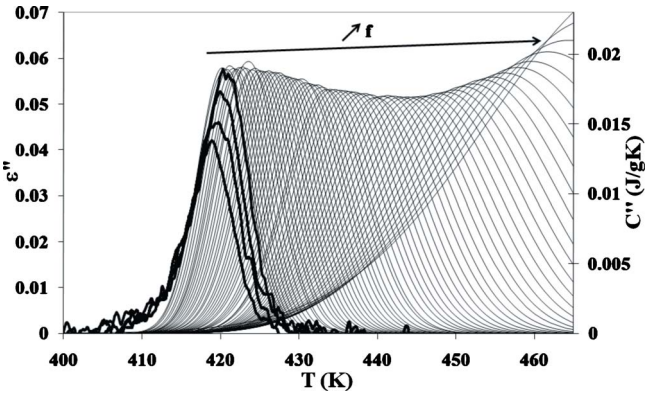

FIG. 5. (Color online) Superposition of the loss peaks obtained by TMDSC (thick line) and BDS (thin line) for PC.

Gaussian fitted to the data. From that data the mean volume of the CRR are calculated by Eq. (1). The determination of the CRR size from Eq. (3) needs the knowledge of the specific-heat capacity in the glassy and in the liquid state. Therefore, the heat capacity values are linearly extrapolated to the dynamic glass transition temperature T_α for each frequency. The TMDSC results are reported in Table II for both samples. As expected, the cooperativity volume increases for both samples when the oscillation frequency decreases, i.e., the dynamic glass transition temperature T_α approaches the thermal one (T_g). These results are in agreement with those obtained in literature concerning the evolution of the cooperativity with temperature [13,14,16–18].

For PC and PETg dielectric loss spectra are presented in Figs. 3 and 4, respectively. For both samples the α relaxation peaks, broadens and shifts toward higher temperatures when the frequency increases. The conductivity phenomenon (ρ) at high temperature and low frequency is also observed in this raw data. Especially for PETg the conductivity contributions are rather strong and circumvent a reliable analysis of the dielectric data at lower frequencies. Moreover for the PETg sample, another loss peak is observed, characteristic of localized β relaxation.

The loss peaks obtained from TMDSC and BDS are superimposed on Figs. 5 and 6 for PC and PETg, respectively. It is worth to notice that the loss peaks increase continuously

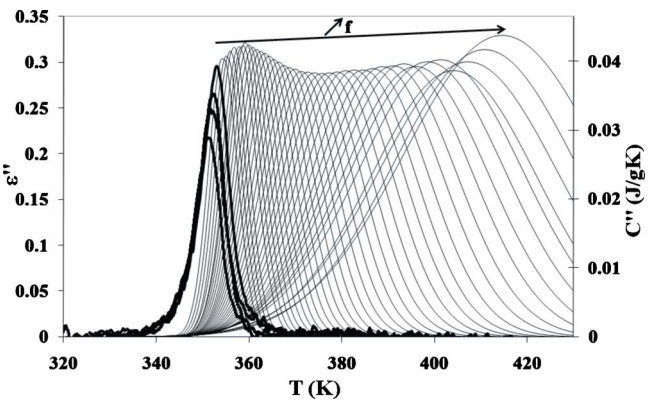

FIG. 6. (Color online) Superposition of the loss peaks obtained by TMDSC (thick line) and BDS (thin line) for PETg

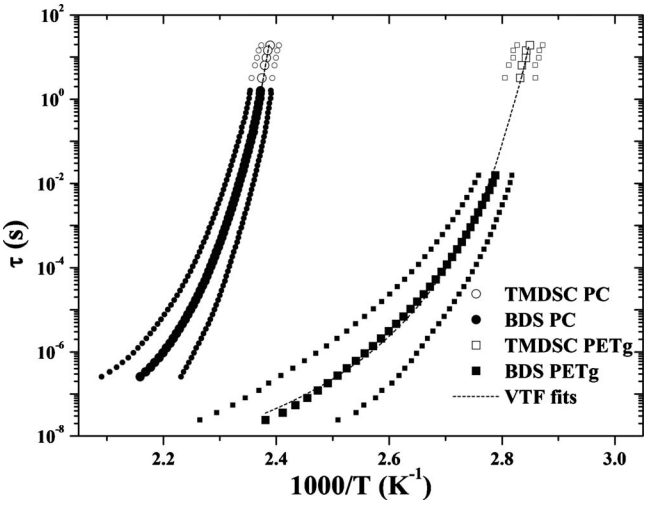

FIG. 7. Evolution of the relaxation time and the dispersion zone as a function of the dynamic glass transition temperature in an Arrhenius plot as deduced from BDS and TMDSC experiments. Dashed lines represent the fit of the VFT equation to the corresponding data for each polymer.

in temperature and in broadness with increasing frequency. This indicates that the suggested analysis procedure seems to be reasonable.

IV. DISCUSSION

To check the equivalence and continuity between the two techniques in terms of relaxation time, the relaxation time deduced from applied frequency for BDS and TMDSC experiments ($\tau = 1/2\pi f$) is plotted as a function of temperature in an Arrhenius plot (Fig. 7). VFT formula is fitted to the data [4–6]

$$\tau = \tau_0 \exp\left(\frac{B}{T - T_0}\right), \tag{16}$$

with τ_0 the pre-exponential factor, B a fitting parameter, and T_0 the so-called Vogel or ideal glass transition temperature which is approximately equivalent to the Kauzmann temperature T_K [47]. The values of the estimated parameters are given in Table III and are similar to those obtained from the BDS experiments [48–50] and also with literature data [36].

As discussed in the introduction the temperature dependence of the relaxation time can be considered as one crucial point of glassy dynamics. The comparison of the relaxation data obtained by these two different probes gives similar and consistent results for $\tau(T)$. The comparison of the CRR size

TABLE III. Values of VTF parameters obtained by fitting the VFT equation to the data of PC and PETg.

Sample	τ_0 (s)	B (K)	T_K (K)
PC	4.3×10^{-11}	616	318
PETg	2.5×10^{-12}	813	392

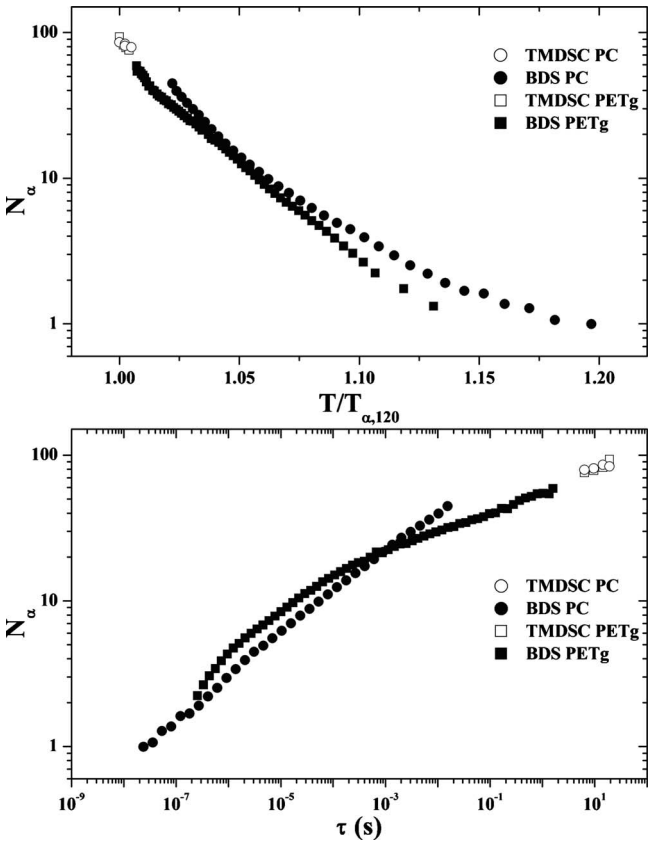

FIG. 8. (Top) Evolution of the number of monomers in a CRR, N_α versus temperature normalized by $T_{\alpha,120}$ for PC and PETg, as deduced from BDS and TMDSC experiments. The temperature is normalized to T_α measured with TMDSC, for a 120 s period. (Bottom) Evolution of the normalized number of monomers in an average CRR, N_α versus relaxation time

calculated by both techniques also requires the comparison of their dissipation zone. Therefore, the dissipation zone of the α relaxation, $(T_\alpha - \delta T) \leq T \leq (T_\alpha + \delta T)$, for PETg and PC are included in Fig. 7. As already obvious from the raw data (see Figs. 5 and 6), a good continuity concerning the evolution of the dissipation zone with the frequency by both spectroscopic techniques (HCS and BDS) is observed in Fig. 7. This is an interesting point considering the fact that it is not a general trend for all the techniques [18]. A strong decrease in δT is observed for both polymers as T_α is decreasing to approach T_g. The resulting calculated values for N_α are shown versus both reduced temperature and relaxation time in Fig. 8. As expected N_α increases with decreasing temperature and/or increasing relaxation time.

The Fig. 8 (top) presents the dependence of the number of particles N_α in one CRR versus a normalized temperature, $T/T_{\alpha,120}$ (with $T_{\alpha,120}$ taken from TMDSC measurement for a period of 120 s which is close to T_g), for PC and PETg. First, the values for N_α calculated from TMDSC and BDS data seem have an extremely good consistency. This regards both its absolute values and its temperature dependence.

Moreover with good consistence in the dependencies of $\tau(T)$ and $\delta(T)$ (cf. Fig. 7), the values of N_α estimated by the two different probes seems to be correlated with the same cooperativity behavior in terms of molecular mobility. As

discussed in the introduction part, even if the microscopic "observables" for these two spectroscopic techniques are different, the measurements done in the dynamic glass transition temperature domain present temperature and polarization fluctuations with similar spectral shape functions $f_T(\omega) \approx f_\chi(\omega)$.

Another worth to notice is that N_α increases in very different ways for both glass-formers. As known in literature [18] and also predicted by the mode-coupling theory, the increase in the number of dynamically correlated particles in the temperature range from the onset of slow dynamics down to T_g, can be described by two regimes: a steeper initial growth for short relaxation times (τ_α) and a much weaker dependence when the temperature approaches T_g. If one analyze the dependence of N_α on the relaxation time in Fig. 8 (bottom), one find that PETg has a unique behavior while PC obeys the discussed two regime dependence.

Another point concerns the temperature range corresponding to the onset of the dynamic glass transition this means the cooperativity phenomenon (N_α is then equal to 1 according to Donth) is approximately $1.15 \leq T/T_\alpha \leq 1.20$ for both polymers. This temperature range corresponds to the classically observed crossover temperature domain in agreement with literature data [35,51–53].

V. CONCLUSION

The temperature dependence of the characteristic length scales associated to the glass transition, such as the cooperativity length scale, is an important tool in studying molecular mobility. In this work, we show that the correlation between BDS and HCS techniques allows to explore a large frequency range and to study the temperature dependence of the size of the CRR in the temperature range of ergodicity loss for glass-forming liquids, starting from the onset of cooperativity in the crossover region down to the glass transition temperature. Finally, the temperature range corresponding to the classically observed crossover temperature domain can be estimated by this way.

ACKNOWLEDGMENTS

We would like to acknowledge Professor Gisèle Boiteux from LMPB-UMR CNRS 5223, University Claude Bernard Lyon I, France, and Professor Colette Lacabanne L2P, Institut CARNOT-CIRIMAT-UMR CNRS 5085, University of Toulouse, France, to give us the opportunity to make the BDS experiments.

[1] E. Donth, *The Glass Transition Relaxation Dynamics in Liquids and Disordered Materials* (Springer, Berlin, 2001).
[2] S. H. Glarum, J. Chem. Phys. **33**, 639 (1960).
[3] G. Adam and J. H. Gibbs, J. Chem. Phys. **43**, 139 (1965).
[4] H. Vogel, Phys. Z. **22**, 645 (1921).
[5] G. S. Fulcher, J. Am. Ceram. Soc. **8**, 339 (1925).
[6] G. Tammann and G. Hesse, Z. Anorg. Allg. Chem. **156**, 245 (1926).
[7] F. Kremer and A. Schönhals, *The Scaling of the Dynamics of Glasses and Supercooled Liquids in Broadband Dielectric Spectroscopy*, edited by F. Kremer and A. Schönhals (Springer, Berlin, 2002), p. 99.
[8] A. Schönhals, Europhys. Lett. **56**, 815 (2001).
[9] F. Garwe, A. Schönhals, H. Lockwenz, M. Beiner, K. Schröter, and E. Donth, Macromolecules **29**, 247 (1996).
[10] W. Götze, *Complex Dynamics of Glass-Forming Liquids: A Mode-Coupling Theory* (Oxford University Press, Oxford, 2008).
[11] S. Capaccioli, G. Ruocco, and F. Zamponi, J. Phys. Chem. B **112**, 10652 (2008).
[12] G. Dlubek, J. Non-Cryst. Solids **352**, 2869 (2006).
[13] O. Yamamuro, I. Tsukushi, A. Lindqvist, S. Takahara, M. Ishikawa, and T. Matsuo, J. Phys. Chem. B **102**, 1605 (1998).
[14] D. Cangialosi, A. Alegria, and J. Colmenero, Phys. Rev. E **76**, 011514 (2007).
[15] C. A. Solunov, J. Phys.: Condens. Matter **14**, 7297 (2002).
[16] H. Zapolsky, A. Saiter, and H. Solunov, J. Optoelectron. Adv. Mater. **91** 141 (2007).
[17] L. Berthier, G. Biroli, J.-P. Bouchaud, L. Cipelletti, D. El Masri, D. L'Hôte, F. Ladieu, and M. Pierno, Science **310**, 1797 (2005).
[18] C. Dalle-Ferrier, C. Thibierge, C. Alba-Simionesco, L. Berthier, G. Biroli, J.-P. Bouchaud, F. Ladieu, D. L'Hôte, and G. Tarjus, Phys. Rev. E **76**, 041510 (2007).
[19] F. Ladieu, C. Thibierge, and D. L'Hôte, J. Phys.: Condens. Matter **19**, 205138 (2007).
[20] E. Donth, E. Hempel, and C. Schick, J. Phys.: Condens. Matter **12**, L281 (2000).
[21] M. Reading and D. J. Hourston, *Modulated-Temperature Differential Scanning Calorimetry: Theoretical and Practical Applications in Polymer Characterisation* (Springer, Dordrecht, 2006).
[22] H. Nyquist, Phys. Rev. **32**, 110 (1928).
[23] H. B. Callen and T. A. Welton, Phys. Rev. **83**, 34 (1951).
[24] T. A. Tran, S. Said, and Y. Grohens, Composites, Part A **36**, 461 (2005).
[25] C. Lixon, N. Delpouve, A. Saiter, E. Dargent, and Y. Grohens, Eur. Polym. J. **44**, 3377 (2008).
[26] N. Delpouve, A. Saiter, J. Mano, and E. Dargent, Polymer **49**, 3130 (2008).
[27] K. Schröter, J. Therm Anal. Calorim. **98**, 591 (2009).
[28] N. O. Birge and S. R. Nagel, Phys. Rev. Lett. **54**, 2674 (1985).
[29] T. Christensen, J. Phys. (France) **12**, C8 (1985).
[30] D. Jung, T. Kwon, D. Bae, I. Moon, and Y. H. Jeong, Meas. Sci. Technol. **3**, 475 (1992).
[31] H. Gobrecht, K. Hamann, and G. Willers, J. Phys. E **4**, 21 (1971).
[32] M. Reading, TRIP **1**, 248 (1993).
[33] H. Huth, A. Minakov, and C. Schick, J. Polym. Sci., B, Polym. Phys. **44**, 2996 (2006).
[34] A. R. Brás, M. Dionísio, H. Huth, Ch. Schick, and A. Schönhals, Phys. Rev. E **75**, 061708 (2007).

[35] A. Schönhals, Ch. Schick, H. Huth, B. Frick, M. Mayorova, and R. Zorn, J. Non-Cryst. Solids **353**, 3853 (2007).
[36] J. Korus, E. Hempel, M. Beiner, S. Kahle, and E. Donth, Acta Polym. **48**, 369 (1997).
[37] H. Huth, M. Beiner, and E. Donth, Phys. Rev. B **61**, 15092 (2000).
[38] H. Huth, M. Beiner, S. Weyer, M. Merzlyakov, C. Schick, and E. Donth, Thermochim. Acta **377**, 113 (2001).
[39] C. Schick, in *Temperature Modulated Differential Scanning Calorimetry–Basics and Applications to Polymers in Handbook of Thermal Analysis and Calorimetry*, edited by S. Cheng (Elsevier, New York, 2002), Vol. 3, p. 713.
[40] S. Weyer, A. Hensel, and C. Schick, Thermochim. Acta **304-305**, 267 (1997).
[41] L. Carpentier, O. Bustin, and M. Descamps, J. Phys. D **35**, 402 (2002).
[42] M. Reading and R. Luyt, J. Therm. Anal. Calorim. **54**, 535 (1998).
[43] D. Boese and F. Kremer, Macromolecules **23**, 829 (1990).
[44] S. Havriliak and S. J. Havriliak, *Dielectric and Mechanical Relaxation in Materials* (Hanser, Munich, Germany, 1997).
[45] O. Bustin and M. Descamps, J. Chem. Phys. **110**, 10982 (1999).
[46] S. Weyer, H. Huth, and C. Schick, Polymer **46**, 12240 (2005).
[47] W. Kauzmann, Chem. Rev. **43**, 219 (1948).
[48] L. Delbreilh, E. Dargent, J. Grenet, J.-M. Saiter, A. Bernès, and C. Lacabanne, Eur. Polym. J. **43**, 249 (2007).
[49] H. Couderc, A. Saiter, J. Grenet, J. M. Saiter, G. Boiteux, E. Nikaj, I. Stevenson, and N. D'Souza, Polym. Eng. Sci. **49**, 836 (2009).
[50] L. Delbreilh, M. Negahban, M. Benzohra, C. Lacabanne, and J. M. Saiter, J. Therm. Anal. Calorim. **96**, 865 (2009).
[51] C. A. Angell, J. Non-Cryst. Solids **131-133**, 13 (1991).
[52] C. A. Angell, B. E. Richards, and V. Velikov, J. Phys.: Condens. Matter **11**, A75 (1999).
[53] A. Schönhals, F. Kremer, A. Hofmann, E. W. Fischer, and E. Schlosser, Phys. Rev. Lett. **70**, 3459 (1993).